# $K^+$-Dependent Composite Gating of the Yeast $K^+$ Channel, Tok1

Stephen H. Loukin and Yoshiro Saimi

Laboratory of Molecular Biology, University of Wisconsin, Madison, Wisconsin 53706 USA

ABSTRACT *TOK1* encodes an outwardly rectifying $K^+$ channel in the plasma membrane of the budding yeast *Saccharomyces cerevisiae.* It is capable of dwelling in two kinetically distinct impermeable states, a near-instantaneously activating R state and a set of related delayed activating C states (formerly called $C_2$ and $C_1$, respectively). Dwell in the R state is dependent on membrane potential and both internal and external $K^+$ in a manner consistent with the $K^+$ electrochemical potential being its determinant, where dwell in the C states is dependent on voltage and only external $K^+$. Whereas activation from the C states showed high temperature dependencies, typical of gating transitions in other *Shaker*-like channels, activation from the R state had a temperature dependence nearly as low as that of simple ionic diffusion. These findings lead us to conclude that although the C states reflect the activity of an internally oriented channel gate, the R state results from an intrinsic gating property of the channel filter region.

## INTRODUCTION

The outwardly rectifying, $K^+$-selective current of the plasma membrane of the budding yeast *Saccharomyces cerevisiae* was first characterized over a decade ago (Gustin et al., 1986). An open reading frame from the yeast genomic database (Miosga et al., 1994) was identified as the gene encoding the ion channel responsible for this current, *TOK1* (Ketchum et al., 1995) (also known as *YKC1* (Zhou et al., 1995), *DUK1* (Reid et al., 1996), and *YORK* (Lesage et al., 1996)). Yeast cells containing deletions of *TOK1* completely lack the outwardly rectifying plasma membrane $K^+$ current, and this current can be restored by expressing *TOK1* in *trans* (Zhou et al., 1995). When expressed in *Xenopus* oocytes, Tok1 induces substantial outward currents that have properties similar to those of the natively expressed channel (Reid et al., 1996). Conceptual translation and hydropathy analysis of the *TOK1* ORF indicates a core topological structure homologous to those of other voltage- and ligand-gated cation channels, namely six membrane-spanning domains, M1–M6, with a conserved semi-hydrophobic P-region between M5 and M6. Two additional membrane-spanning domains surround a second P-region, giving Tok1 a predicted overall M1–5-P1-M6–7-P2-M8 structure.

The rectification of Tok1 was originally described as transmembrane voltage ($V_m$) dependent (Gustin et al., 1986). Based on the effects of substituting external $K^+$, Ketchum et al. (1995) concluded that Tok1's rectification is not determined by $V_m$ directly, but by offset from the $K^+$ equilibrium potential ($V_m - E_K$). These same authors proposed that an external divalent ion block is responsible for this apparently $E_K$-dependent rectification, but subsequent attempts to corroborate this result were unsuccessful (Lesage et al., 1996; Zhou et al., 1995). Other authors have concluded that external $K^+$ most likely affects rectification through allosteric effects of $K^+$ binding on gating (Bertl et al., 1998; Vergani et al., 1997). In none of these experiments, though, were the effects of internal $K^+$ concentration ($[K^+]_{int}$) assessed.

Tok1 activates both with seemingly instantaneous and delayed kinetics upon depolarization (Ketchum et al., 1995) and deactivates with seemingly instantaneous kinetics upon repolarization, leading to the proposal by Lesage et al. (1996) of a serial $C_1 \leftrightarrow C_2 \leftrightarrow O$ state model in which the $C_1$-$C_2$ transition is slow and the $C_2$–O transition is instantaneous. Steady-state distribution into $C_1$ (which in fact is a set of related but kinetically distinct closed states) is favored by high external $K^+$ concentration ($[K^+]_{ext}$) and negative $V_m$, but the effect of internal $K^+$ concentration ($[K^+]_{int}$) on this distribution was not tested here as well (Loukin et al., 1997). Mutations in the cytoplasmic juncture of either M6 or M8 largely eliminate $C_1$, leaving $C_2$ states intact, indicating the importance of these regions in determining $C_1$ and the independence of $C_1$ from $C_2$. These $C_1$-deficient mutant channels have wild-type steady-state current/voltage ($I/V$) relationships, indicating that $C_2$ alone is sufficient for imparting steady-state outward rectification (Loukin et al., 1997).

In this report we investigate the effect of varying $[K^+]_{int}$ and $[K^+]_{ext}$ on both steady-state rectification and $C_1/C_2$ distribution. We also analyze the effect of temperature on current activations to investigate the nature of the mechanisms underlying both $C_1$ and $C_2$. We conclude that whereas the $C_1$ results from a closing of an internally oriented channel gate in response to the allosteric binding of external $K^+$, $C_2$ reflects a $K^+$-electrochemical-potential-dependent intrinsic gating property of the channel filter region. To underscore their difference we refer to $C_2$ as "R," for "rectifying," and $C_1$ as simply "C." We postulate and, in one case, mathematically test specific hypothetical models of

*Received for publication 5 February 1999 and in final form 2 September 1999.*

Address reprint requests to Dr. S. H. Loukin, Laboratory of Molecular Biology, University of Wisconsin, 1525 Linden Dr., Madison, WI 53706; Tel.: 608-262-7976; Fax: 608-262-4570; E-mail: shloukin@facstaff.wisc.edu.



0006-3495/99/12/3060/11 $2.00

how the channel's selectivity filter region could intrinsically gate in response to the $K^+$ electrochemical potential.

## MATERIALS AND METHODS

### Oocyte expression of Tok1

Expression of Tok1 in *Xenopus* oocytes was as described in Loukin et al., 1997.

### Macro patch clamp recording

Three to seven days after RNA injections, oocytes were prepared for patch clamp recording by removal of the vitelline membrane as described in Loukin et al. (1997). Inside-out patches were sealed to flame-polished macro-patch pipettes having bore diameters between 5 and 20 $\mu$m. Currents were recorded using a GeneClamp 5500 patch clamp amplifier with a CV-5–1GU headstage interfaced through a DigiData 1200 digital-to-analog converter to a standard PC running pClamp6 or Clampex7 software (all except PC, Axon Industries Inc., Foster City, CA). Data were sampled at 2 ms and filtered at 5 kHz at the point of acquisition. Bath solutions were changed by moving patches between continuously flowing perfusates in a multi-welled chamber. Junction potentials, which were compensated for before seal formation in symmetrical $K^+$, were rechecked at the end of experiments and were found never to vary more than $\pm$3 mV. Data were analyzed using a combination of pClamp6, Origin 4.1 (Microcal Software Inc., Northampton, MA) and Sigma Plot 4 for Windows (SPSS Software Inc., Chicago, IL). Except where stated, neither leak subtraction nor capacitance compensation was used at the point of data acquisition or analysis.

### Whole oocyte recording

Two to seven days after injections, two electrode voltage clamp experiments were performed using a GeneClamp 500 amplifier with HS-2A headstages and a VG-2A virtual ground bath clamp interfaced through a DigiData 1200 digital-to-analog converter to a standard PC running pCLAMP6 or Clampex7 software. Low resistance electrodes were used that had 15–25-$\mu$m bores containing 2M KCl, and 2% agarose at their tips based on previously described methods (Schreibmayer et al., 1994). Data in standard recordings were sampled at 5 kHz and filtered at 1 kHz at the point of acquisition. For analysis of the O-R kinetics, data were sampled at 167 kHz, filtered at 50 kHz, and stabilization was set at the minimum, which prevented severe ringing (generally a phase lag of 20 $\mu$s). Temperature was controlled using a Cambion Bipolar Temperature Controller (Midland Ross Inc., Urbana, OH) and monitored by measuring calibrated current flow through a small thermocouple placed near the oocyte. Neither leak subtraction nor capacitance compensation was used at the point of data acquisition or analysis unless stated.

## RESULTS

### $\Delta\mu_{K^+}$ Dependence of steady-state rectification

The $K^+$ and $V_m$ dependence of steady-state rectification of oocyte-expressed Tok1 was determined by measuring currents passing through inside-out macropatches at differing external and internal $K^+$ concentrations ($[K^+]_{ext}$ and $[K^+]_{int}$) during voltage ramps slowly increasing between $-90$ and $+90$ mV. Current/voltage (*I/V*) relationships were examined at $[K^+]_{ext}/[K^+]_{int}$ of 1.4/140 (▲□), 14/140 (●□), 140/140 (■□), and 140/14 (■○) mM (Fig. 1 *A*). Viewed on current scales necessary to visualize the outward current/voltage profile, inward current is not evident. When viewed on an expanded current axis (Fig. 1 *A, inset*), current reversals can in fact be observed at voltages of $-47 \pm 2$ ($n = 3$), $-1 \pm 2$ ($n = 4$), and $46 \pm 2$ ($n = 4$) in 14/140, 140/140, and 140/14 mM $[K^+]_{ext}/[K^+]_{int}$, respectively. These reversal potentials ($E_{rev}$ values) are near the predicted $K^+$ equilibrium potentials ($E_K$ values) as expected for a $K^+$ selective channel.

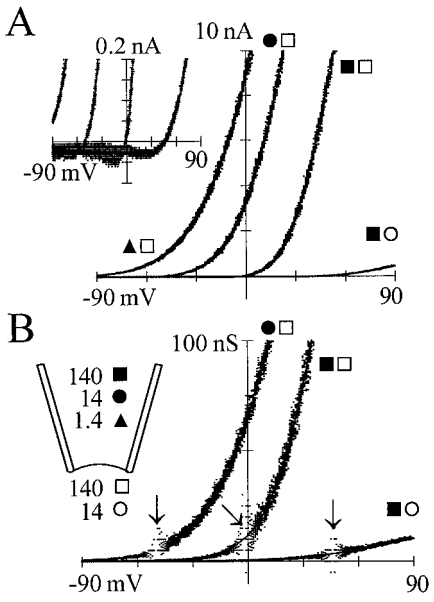


FIGURE 1 Rectification of Tok1 with varying $[K^+]_{ext}$ and $[K^+]_{int}$. (*A*) Currents were measured in response to slow (17 s) voltage ramps between $-90$ and $+90$ mV from inside-out macropatches excised from oocytes expressing high levels of Tok1. The pipette contained 140 (■), 14 (●), or 1.4 (▲) mM KCl and the bath contained either 140 (□) or 14 (○) mM KCl (N-methyl D-glucamine ($NMG^+$) chloride was added as necessary to keep the total $[K^+]$ + $[NMG^+]$ at 140 mM). The two 140 mM $[K^+]_{ext}$ traces are from the same patch. Measured currents are plotted without leak subtraction against $V_m$, which is monitored by the simultaneous measurement of pipette potential. In the inset, the same four current records are plotted on an amplified current scale to show reversals. (*B*) Chord conductance (*G*)/*V* relationships calculated from the traces in *A* divided by the offset from the observed current reversal for that trace (*arrows*). The 1.4 mM $[K^+]_{ext}$ could not be plotted because a reversal in these conditions was not observed. In addition to KCl and NMG-Cl, bath solutions also contained 1 mM $CaCl_2$, 4 mM $MgCl_2$, 5 mM EGTA, and 5 mM HEPES, pH 7.5. Pipette solutions were similar but lacked EGTA and contained only 1 mM $MgCl_2$. The *I/V* relationships illustrated in this figure are typical of those repeatedly observed in independent experiments ($n \geq 4$). Similar results were obtained when $Na^+$ was used in place of $NMG^+$.

Chord conductance (*G*) plots were constructed based on the offset from the observed $E_{rev}$ values. In symmetrical 140 mM $K^+$, little conductance was observed below the reversal potential of 0 mV (Fig. 1 *B*, ■□, arrow points to $E_{rev}$). Substantial conductance is observed from 0 down to $-50$ mV when $[K^+]_{ext}$ is reduced to 14 mM (●□), though. This change in conductance between $-50$ and 0 mV must be attributed to a change in the permeability of Tok1, not a change in conducting ion concentration, because the same 140 mM $K^+$ is present on the side from which $K^+$ ions would tend to flow in both cases. Arguing against a purely

allosteric effect of $K^+$ on gating is the observation that $[K^+]_{int}$ has the opposite effect on conductance as $[K^+]_{ext}$: whereas substantial conductance is observed between 0 and +50 mV in symmetrical 140 mM $K^+$ (Fig. 1 *B*, ■□) little or no conductance is seen in this same voltage range when $[K^+]_{int}$ is reduced to 14 mM by bath perfusion (■○). As before, this lack of conductance between 0 and 50 mV cannot be explained by a lack of permeant ion, which is 140 mM in both cases (though the notable decrease in conductance above $E_{rev}$ can be attributed to the 10-fold reduction in $[K^+]_{int}$). $K^+$ was substituted with N-methyl D-glucamine ($NMG^+$) in Fig. 1, but replacing $K^+$ with $Na^+$ had an effect similar to $NMG^+$ (not shown; Bertl et al., 1998), demonstrating the specificity of the effect of $K^+$ on rectification.

It is clearly the ratio of internal to external $K^+$, not absolute $K^+$ concentrations, that determines Tok1 conductance. The profiles of $I_{standardized}/V$ plots consistently overlap as long as the $[K^+]_{int}/[K^+]_{ext}$ ratios are similar (Fig. 2). Substantial current first appears just positive to $E_K$ and increases with positive-going voltage at a similar rate irrespective of the absolute $K^+$ concentrations. Thus Tok1 conductance appears to be determined by the electrochemical driving force for $K^+$, $\Delta\mu_{K^+}$. It should be noted that at highly positive membrane potentials (>100 mV) there was an apparent $V_m$-dependent decrease in conductance (data not shown). We conclude, though, that the onset of conductance in physiological voltage range is more significant, and we thus refer to the steady-state rectification of Tok1 as being $\Delta\mu_{K^+}$-dependent.

## Time dependence of R/O transitions

Upon depolarization from mildly negative holding potentials, a substantial fraction of Tok1 current activates with seemingly instantaneous kinetics, reflecting transition from the R to O state (Fig. 3 *A*, "R → O"). Although rapid, the kinetics of activation from the R state can in fact be discerned if techniques are used to minimize the duration of the capacitive spike (see Methods). In such experiments the outward capacitive current had abated and the cytoplasmic potential measured at the non-current injecting electrode had reached the command potential by <0.2 ms after a voltage step from −20 mV to between +60 and +80 mV (Fig. 3 *B, dotted line*). Current is still increasing well beyond this point (*right of dotted line*) reflecting an increase in membrane conductance due to the R to O transition. Monoexponential fitting of such transitions after subtraction of capacitive currents revealed activation $\tau$ values between 0.1 and 0.3 ms (see below).

When repolarized, Tok1 currents likewise relax with apparently instantaneous kinetics reflecting the transition from the O to R state (Fig. 3 *A*, "O → R"). Discerning the O-R transition is more difficult than above because both the capacitive and deactivating currents are relaxing at the point of analysis, and therefore the Tok1 component is not as qualitatively obvious as during activation. The capacitive component of the composite inward current observed upon repolarization in the presence of 100 mM external $K^+$ (Fig. 4 *A*) can be discerned by repeating the voltage protocol after removing most of the external $K^+$ by perfusion (Fig. 4 *B*). Only insignificant inward Tok1 current will be present in the latter case due to a lack of permeant ion in the external solution. Subtracting the 1 mM external $K^+$ trace from the 100 mM $K^+$ trace reveals the deactivating Tok1 current (Fig. 4 *C*). Monoexponential fitting revealed that Tok1 migrates from the O to the R state with a $\tau$ of 0.22 ± 0.05 ms (mean ± SD, $n = 4$). That this extrapolated inward current indeed reflects Tok1 activity is demonstrated by the

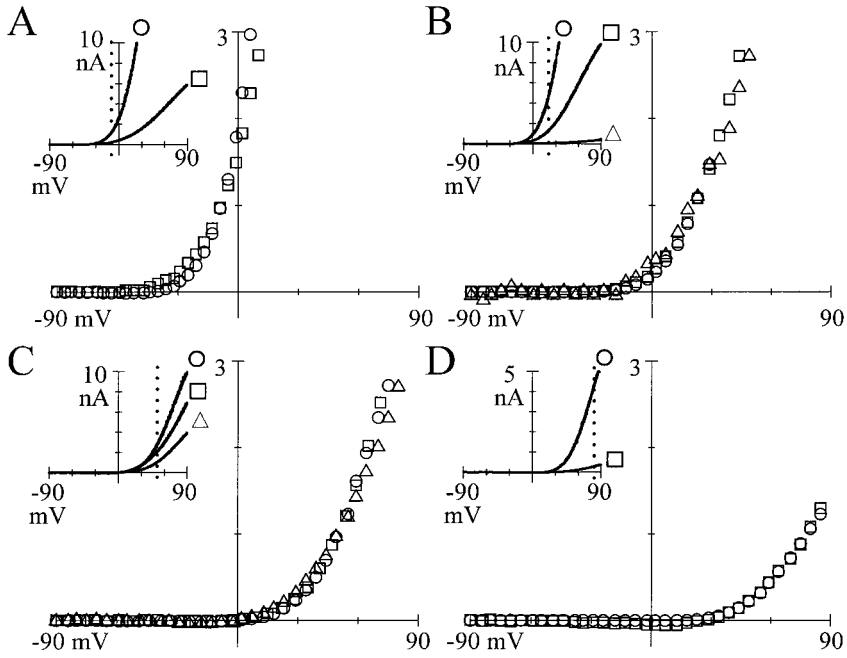


FIGURE 2 Comparison of *I/V* relationships at identical $[K^+]_{int}/[K^+]_{ext}$ ratios. Currents were measured from Tok1 expressing oocyte macropatches as in Fig. 1 in $[K^+]_{ext}$ varying from 1.4 to 140 mM and $[K^+]_{int}$ varying between 14 mM and 140 mM. These traces are presented such that each plot contains traces of differing absolute $K^+$ concentrations but identical $[K^+]_{int}/[K^+]_{ext}$ ratios. The inset in each trace shows the raw current traces and the main plots show these traces normalized at a value 50 mV positive to $E_K$ (*dashed line in insets*). (*A*) *I/V* relationships in $[K^+]_{int}/[K^+]_{ext}$ of 10/1: 140/14 (○) and 44/4.4 (□) (all $K^+$ concentrations are given as $[K^+]_{int}/[K^+]_{ext}$ in mM). Current could not be observed in the presence of 14 mM/1.4 mM $[K^+]_{int}/[K^+]_{ext}$. (*B*) $[K^+]_{int}/[K^+]_{ext}$ of 3.2/1: 140/44 (○), 44/14 (□), and 14/4.4 (△). (*C*) Symmetrical $[K^+]$: 140/140 (○), 44/44 (□), 14/14 (△). (*D*) $[K^+]_{int}/[K^+]_{ext}$ of 1/3.2: 140/44 (○) and 44/14 (□). Other solution components and recording conditions were as in Fig. 1.

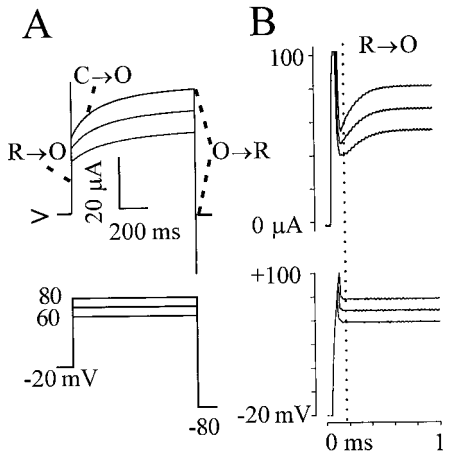


FIGURE 3 Time dependence of R to O transition. (*A*) When whole oocytes are depolarized from −20 mV in 100 mM KCl bath solutions, outward Tok1 currents surge at two qualitatively distinct rates, reflecting an apparently instantaneous "R → O" transition and a delayed "C → O" transition. The horizontal caret marks the 0 current level. Upon repolarization, currents relax at a seemingly instantaneous rate reflecting an "O → R" transition. Note that these traces represent current activity over the course of 1 s. (*B*) When viewed on an ~1000-fold expanded time axis, the time course of the "instantaneous" R → O activation can easily be discerned. The lower plot in *B* is the pipette potential at the voltage-sensing electrode in this two-electrode voltage clamp experiment illustrated on the same time axis to show that the circuitry had charged long before currents had finished surging. Thus the change in current amplitude to the right of the dotted line reflects an increase in membrane conductance due to R to O activation. In addition to the KCl, bath solutions contained 5 mM HEPES, 1 mM $MgCl_2$, and 1 mM $CaCl_2$, pH 7.5.

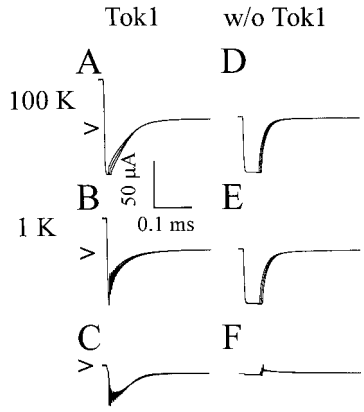


FIGURE 4 Time dependence of O to R deactivation. The inward current in Tok1 expressing whole oocytes (*A–C*) was analyzed immediately upon stepping from a 1 s conditioning pulse of +80 mV to test potentials between −100 and −80 mV in 100 mM (*A*) and 1 mM (*B*) external KCl (note: entire trace is only 0.5 ms; horizontal caret in 1 *A* indicates 0 current level). (*C*) Upon subtraction of the 1 mM from the 100 mM trace, the external-$K^+$-dependent component of the inward current becomes clear. That the decaying inward current in C reflects Tok1's O to R transition is demonstrated by its lack in nonexpressing oocytes (*D–F*). Bath solutions in *B* and *E* were as in Fig. 3 and those in *A* and *D* contained 1 mM KCl, 99 mM NMG-Cl in place of 100 mM KCl (identical results were obtained when NaCl was substituted for NMG-Cl). The presence of this external $K^+$-dependent inward tail current was repeatedly observed in Tok1 expressing oocytes, yet never observed in nonexpressing oocytes ($n \geq 4$ each).

its absence in uninjected oocytes (e.g., Fig. 4, *D–F*, $n = 5$). This inward current is mechanistically significant. It demonstrates that Tok1 can indeed transport $K^+$ inwardly because ~$10^3$ ions would be transported through the average channel over the course of this O to R deactivation, ruling out a diode-like model of Tok1 rectification in which the filter is inherently incapable of conducting $K^+$ inwardly in any state.

## Temperature dependence of activation from the R state

The $\Delta\mu_{K^+}$ dependence of steady-state rectification can be attributed to R/O distribution alone, because genetic disruption of the delayed activating C state does not affect this rectification (Loukin et al., 1997). Also, the rapid cessation of inward current flow upon repolarization is due to migration from O to R, not C (Loukin et al., 1997). Both this $\Delta\mu_{K^+}$ dependence and the rapid nature of the R-O transition raised doubt as to whether it reflected the activity of a deactivation gating mechanism akin to those of other *Shaker*-like channels. Where determined, activation rates of these channels, even the extremely rapid ones, have large temperature dependencies with $Q_{10}$ values between 2 and 4 (Beam and Donaldson, 1983; Collins and Rojas, 1982; Alvarado et al., 1979; Chiu et al., 1979; Schauf, 1973; Moore, 1971; Dudel and Rudel, 1970; Frankenhauser and Moore, 1963; Hodgkin and Katz, 1949), reflecting sizable enthalpic barriers between the open and closed states, indicating a substantial conformational transition. Because the activation rate from the R state could be discerned, its temperature dependence could be assessed.

Initial attempts to assess the temperature dependence of the rapid activation revealed an inexplicable temperature-independent increase in the activation rate over the course of several minutes. To account for this time-dependent increase, activation rates were repeatedly measured at 20° and 30° alternately (typical traces shown Fig. 5, *A* and *B*; only two temperature points were used to facilitate the correction for the temperature-independent rate increase). The $Q_{10}$ of rapid activation, determined as the mean of the rates at 20° to those of the prior and subsequent 30° rates, is 1.4 ± 0.1 (Fig. 5 *C*). This temperature dependence is as low as that of channel conductance and suggests that transition from the R to O state does not involve a substantial conformational rearrangement of the protein as is thought to underlie deactivation gating of other *Shaker*-like channels.

## Temperature dependence of activation from the C states

When depolarized from potentials substantially negative to $E_K$, the majority of outward current surges with delayed kinetics reflecting transition from C. At higher temperatures, it requires three exponents to adequately fit this de-

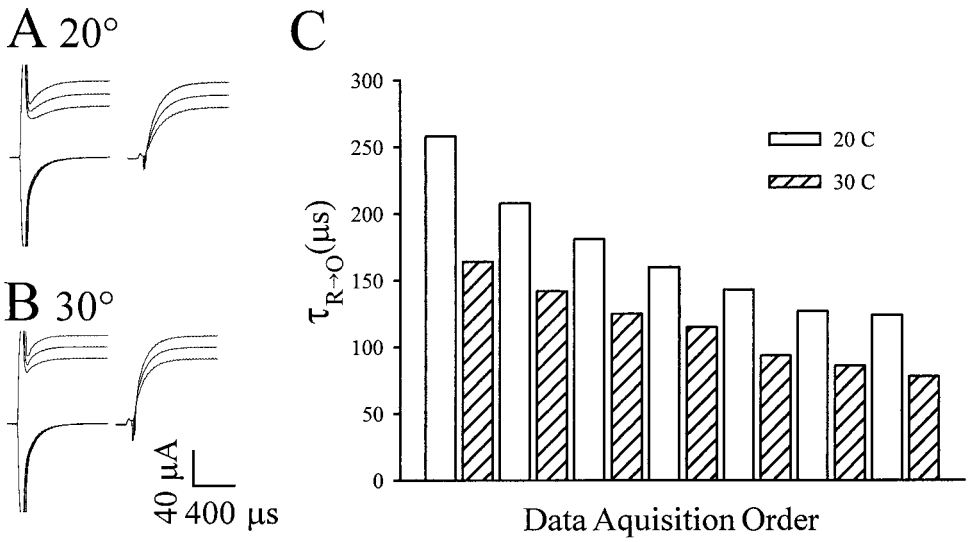


FIGURE 5 Activation rate from R has only a mild temperature dependence. (*A*) Current records from whole oocytes expressing high levels of Tok1 upon stepping from a holding potential of −20 mV to test potentials between +60 and +80 mV and test potentials symmetrically negative from the hold (−100 to −120 mV) recorded at 20°C (note: traces only represent 1 ms). The leftward of the two plots are the raw current records and the rightward shows the result of adding the current occurring upon depolarization to that occurring upon symmetrical hyperpolarization to subtract the capacitive component. (*B*) Analogous currents recorded and extrapolated from the same oocyte at 30°C. (*C*) O to R activation rate constants were determined by single exponential fits of the capacitance-subtracted traces to +80 mV. Activation rates at 20°C were compared to both prior and subsequent rates at 30°C to yield an estimated $Q_{10}$ of R to O activation of 1.4 ± 0.1. Bath solutions were the same as those described in Fig. 3.

layed activation, indicating that C is in fact a set of related closed states: C-slow, C-intermediate, and C-fast. That these states are physically related to each other is indicated by the fact that single point mutations effect all three simultaneously (Loukin et al., 1997). Unlike the case of the R state, activation rates from the C states did not inexplicably increase over the course of experiments. Temperature had a dramatic effect on the conglomerate activation from C (Fig. 6 *A*). This was due to cumulative effects of temperature on both distribution between the various C states and on the activation rates from the individual states themselves. C-slow was favored by low temperature such that at 14°C, C activation occurred almost exclusively from C-slow (Fig. 6 *B*). Activation from C-slow had a $Q_{10}$ of 3.5 between 18° and 26°C (Fig. 6 *D*). That of C-intermediate had a $Q_{10}$ of 3.1 between 20° and 26°C (Fig. 6 *C*). The $Q_{10}$ of C-fast could not be reliably determined, because it was a substantial component only at the highest assayable temperatures. Thus, unlike activation from R, activations from the C states have temperature dependencies typical of those of gating transitions of other ion channels.

## Independence of C-state dwell on $[K^+]_{int}$

Previous whole oocyte experiments showed that distribution into the delayed C states is favored by negative $V_m$ and high $[K^+]_{ext}$ (Loukin et al., 1997; Vergani et al., 1997). Using inside-out macropatches, we assessed the ability of $[K^+]_{int}$ to affect C distribution. Currents were measured under varying $K^+$ conditions from excised macropatches in response to depolarizing steps from holding potentials that varied between −100 and +20 mV (Fig. 7 *A*). Internal $K^+$ was varied by bath perfusion and thus direct comparisons of the effect of $[K^+]_{int}$ on a single patch could be made. It was necessary to use more positive test potentials to monitor activation in 14 mM $[K^+]_{int}$ than in 140 mM $[K^+]_{int}$ due to the dramatically lower current levels resulting from the combined effects of lower permeant ion concentration and decreased offset from $E_{rev}$. At the intermediate $[K^+]_{int}$ of 44 mM, activation could be monitored to both test potentials to ascertain whether the test potential value had an effect on C/R distribution at the holding potential, the parameter being assayed here. It was found that as long as the test potential was significantly above $E_{rev}$ it did not affect the estimation of C distribution, although it did increase the activation rate from C, an effect that was not investigated further.

A compilation of several such experiments, which was necessary due to patch-to-patch variability in C distribution, verified that distribution into C was consistently dependent on both holding potential and $[K^+]_{ext}$ in excised patches similar to its dependence in whole cell recordings (Loukin et al., 1997). A 10-fold reduction in $[K^+]_{ext}$ resulted in an ~−50 mV shift in the C-distribution profile (e.g., compare black to gray or gray to white symbols in Fig. 7 *B*). Distribution into C was not systematically affected by variation of $[K^+]_{int}$, though. Reduction of $[K^+]_{int}$ 10-fold from 140 mM to 14 mM resulted in no consistent shift in the C-distribution profile (compare different symbols of same color in Fig. 7 *B* to each other). Thus, distribution into C is determined by $V_m$ and $[K^+]_{ext}$, but not by $[K^+]_{int}$.

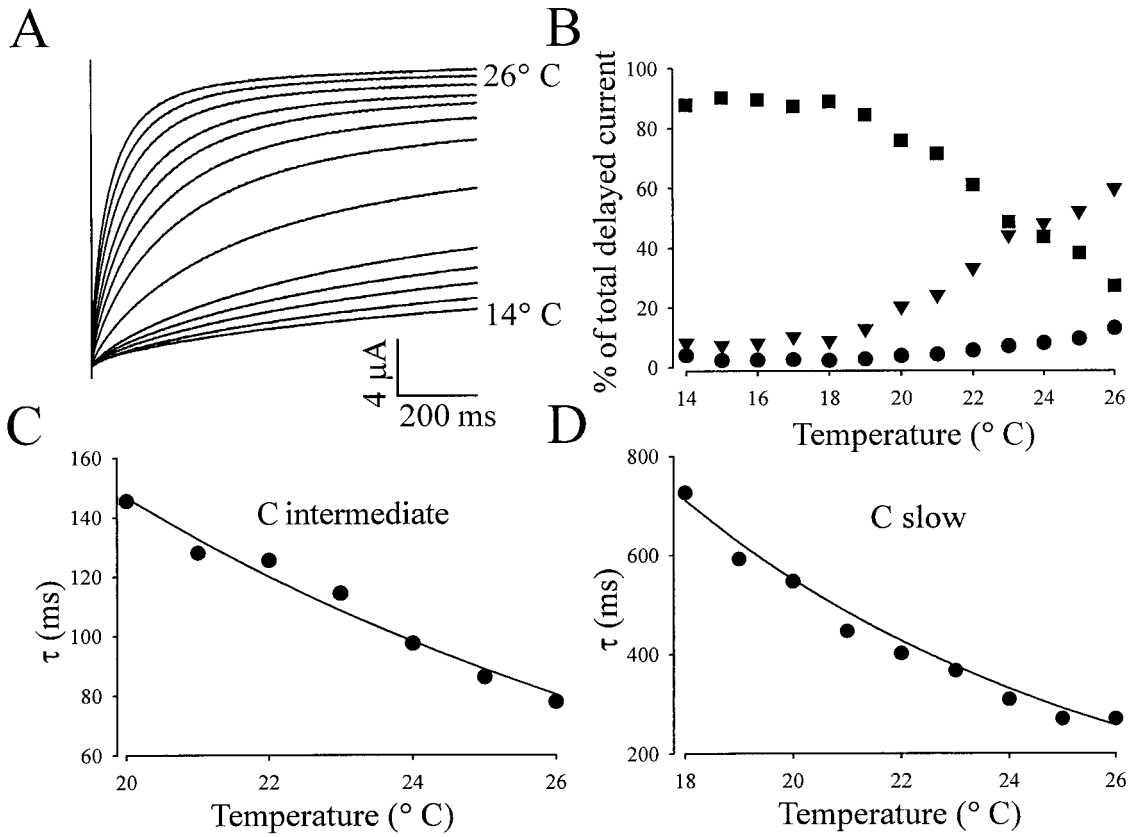


FIGURE 6 Activation rates from C have high temperature dependencies. (*A*) Currents elicited from Tok1 expressing whole oocytes upon depolarization from a holding potential of −80 mV to a test potential of +80 mV at temperatures ranging between 14° and 26° in 1°C intervals. (*B*) The current traces of *A* were fitted between 2 and 900 ms to third-order exponentials, the minimum order necessary to fit the traces at higher temperatures. The fractional magnitude of the fast (●), intermediate (▼), and slow (■) components of such fits are plotted against temperature. (*C*) Activation rates between 20° and 26°C from the intermediate C substate reveal a $Q_{10}$ of 3.1. (*D*) Activation rates between 18° and 26°C have a $Q_{10}$ of 3.5. Bath solutions and recording conditions were as in Fig. 3.

## DISCUSSION

In this work we have shown that the steady-state rectification of Tok1 is primarily dependent on the electrochemical potential for $K^+$ ($\Delta\mu_{K^+}$) and that Tok1 resides in two types of impermeable states, C and R, distinguished not only by kinetics but by temperature sensitivity and $[K^+]_{int}$ dependence. We conclude that whereas the C state results from a conformational occlusion of the inner mouth of the permeation pathway in response to allosteric effects of binding external $K^+$, the R state instead reflects an intrinsic gating property of the channel's filter region. The remainder of this discussion will be devoted to a justification of these conclusions and a postulation of specific mechanisms by which the filter region could intrinsically gate in response to $\Delta\mu_{K^+}$.

### The R state is an intrinsic property of the channel's filter region

The effect of voltage and changes in internal and external $K^+$, but not $Na^+$ or $NMG^+$, demonstrates that Tok1 rectifies specifically in response to the electrochemical potential of $K^+$ and not that of other cations (but, see Bertl et al., 1998). The R state alone can account for this property: C-deficient mutants maintain this seeming $\Delta\mu_{K^+}$-dependent rectification and inward current flow is at least initially prevented by the R state upon negative voltage steps across $E_K$ (Loukin et al., 1997). Thus dwell in the R state is, at least apparently, $\Delta\mu_{K^+}$-dependent. Several models have been proposed to account for the ability of $[K^+]_{ext}$ and voltage to affect the rectification of Tok1.

Vergani et al. (1997) proposed that an externally oriented $K^+$ binding site exists within the membrane field but outside of the permeation pathway binding to which allosterically closes a channel gate. Our finding that increasing $[K^+]_{int}$ affects conductance oppositely to increasing $[K^+]_{ext}$ greatly complicates such schemes in which effective $K^+$ binding occurs outside of the pore, because they would now require the complex coordination of independent allosteric bindings to sites on both sides of the channel. It is far more economical to model the pore as the site of $\Delta\mu_{K^+}$-sensing inasmuch as $\Delta\mu_{K^+}$ would have an obvious influence on $K^+$ binding there because internal and external $K^+$ could have opposite effects by antagonizing each other's bindings through electrostatic repulsion.

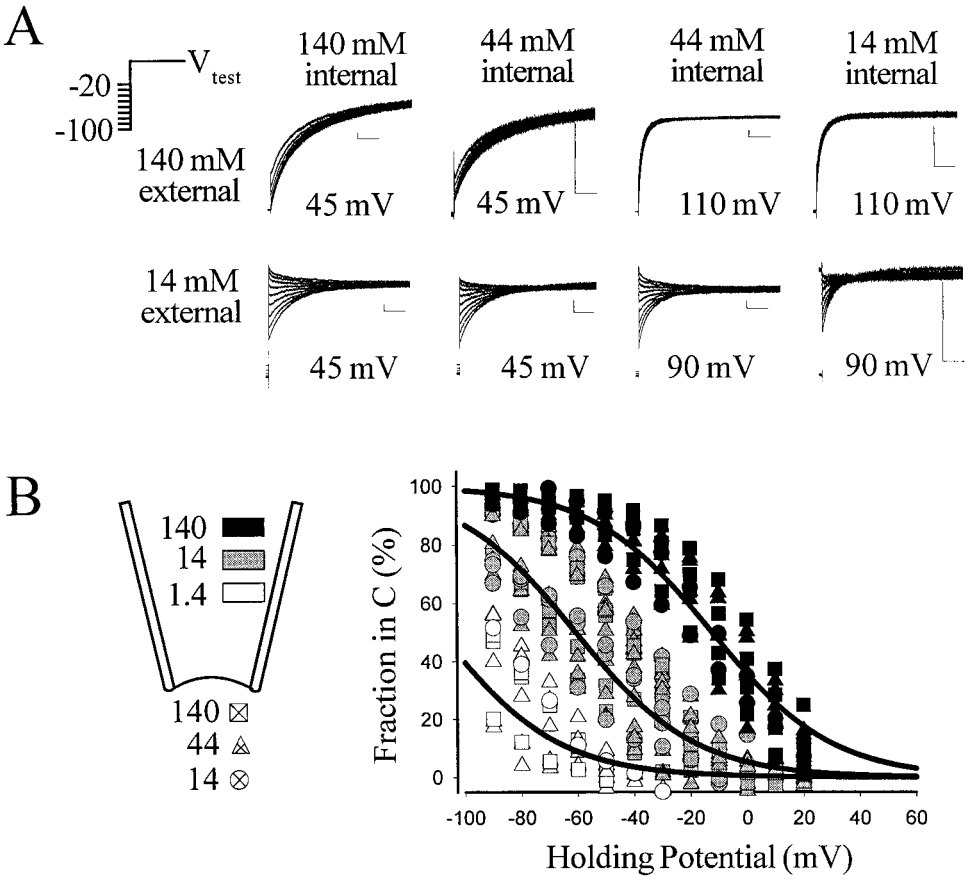


FIGURE 7 Dependence of C dwell on $V_m$, $[K^+]_{ext}$ but not $[K^+]_{int}$. (*A*) Current activations upon stepping to the test potential stated within each plot from holding potentials between −100 and +20 mV were measured through macropatches excised from Tok1 expressing oocytes. The top row shows current traces from a single macropatch exposed to 140 mM external (pipette) KCl and the bottom row from another patch exposed to 14 mM external KCl. Internal $K^+$, which was altered by bath perfusion, is as stated above each column of plots. Other solution components are as described in Fig. 1. Calibration bars represent 500 pA × 200 ms. (*B*) The fraction of the current activating from C as opposed to R was estimated by fitting the raw traces to third-order exponential functions, extrapolating the current values to $t = 0$ and ∞, and dividing the former by the latter then subtracting from 100%. $[K^+]_{ext}$ corresponds to the fill of the symbol being 140 (*black*), 14 (*gray*), or 1.4 (*white*) mM. $[K^+]_{int}$ corresponds to the shape of the symbol being 140 (*squares*), 44 (*triangles*), or 14 (*circles*) mM. Whereas reduction of $[K^+]_{ext}$ causes a consistent decease in C dwell, altering $[K^+]_{int}$ had no systematic effect on C/R distribution. Solid lines represent predictions of C distributions in 1.4, 14, and 140 mM $K^+$ (*left to right*) assuming that C dwell is determined by $K^+$ binding to a single externally accessible site buried 60% across the membrane's electrical field (see Discussion).

Both intrinsic and extrinsic blocking schemes have been proposed as mechanisms by which $K^+$ binding within the permeation pathway could affect Tok1's gating. Ketchum et al. (1995) inferred an external divalent blocking mechanism based on an apparent loss of Tok1 rectification when EDTA is added to the external solution. Subsequent investigations had failed to corroborate this result, though (Lesage et al., 1996; Zhou et al., 1995) and unpublished experiments indicate that this loss of rectification may have resulted from deterioration of the patch seal due to divalent ion chelation (Loukin, unpublished observations). There is no evidence for a role for more complex extrinsic blocking factors such as polyamines in Tok1's rectification because they are not present in the baths, and extensive perfusion of either inner or outer solutions, which should remove soluble cellular factors, does not abolish rectification. Lesage et al. (1996) proposed an intrinsic blocking mechanism in which an externally oriented ball-and-chain type charged blocking domain occludes the permeation pathway. Such a mechanism would require this domain to enter deeply into the pore, most likely well within the filter region itself, because external $K^+$ but not $Na^+$ or $NMG^+$ must "lock" the blocking domain in place and internal $K^+$ must specifically displace it. Assuming that the pore structure of Tok1 is similar to the crystal structure of KcsA, we conclude that steric hindrance would prevent a peptide domain from entering deeply into the filter.

In lieu of a blocking mechanism, $\Delta\mu_{K^+}$-specific sensing must be presumed to directly result from differential effects of internal and external $K^+$ binding. Such binding most likely occurs at the filter region because the sites there are $K^+$-specific, in contact with both the inner and outer solutions, and binding of $K^+$ from one side would antagonize binding of $K^+$ from the other side, thus greatly simplifying a $\Delta\mu_{K^+}$-sensing mechanism. Permeant ion binding to the filter is thought to affect the gating of other ion channels.

There is mounting evidence that $K^+$ binding antagonizes C-type inactivation of *Shaker* by preventing a collapse of the filter (Kiss et al., 1998; Kiss and Korn, 1998; Starkus et al., 1997, 1998). Chloride binding to the filter has been shown to affect closed-state dwell of the ClC-0 chloride channel (Chen and Miller, 1996). In the case of ClC-0, though, only $[Cl^-]_{ext}$ strongly affects closed-state dwell.

Inasmuch as the filter region would have to be exposed to both the inner and outer solutions to "sense" the total transmembrane $\Delta\mu_{K^+}$, either the O to R transition rate alone is $\Delta\mu_{K^+}$-dependent or the filters binding sites must remain at least partially intact and exposed to the inner and outer solutions in the R state. The former case is untenable. O to R deactivation occurs at a rate of $\sim 10^4\ s^{-1}$ at $-100$ mV (Fig. 4). If the R to O activation was $\Delta\mu_{K^+}$-independent, occurring at the same $\sim 10^4\ s^{-1}$ rate at $-100$ mV as it does at $+100$ mV (Fig. 3), then a substantial fraction of the channels should be in the O state at $-100$ mV, which is clearly not the case (most clearly shown with C-deficient mutants (Loukin et al., 1997)). Instead it is necessary to infer the latter case, that the inner and outer $K^+$ binding sites of the nonconducting R state filter remain capable of binding $K^+$ and exposed to the inner and outer solutions, respectively. Thus the R-state "gate" must be intrinsic to the filter region and not reflect an occlusion of the permeation pathway on either side of the filter. We thus conclude that R-state gating is an intrinsic property of the channel filter region.

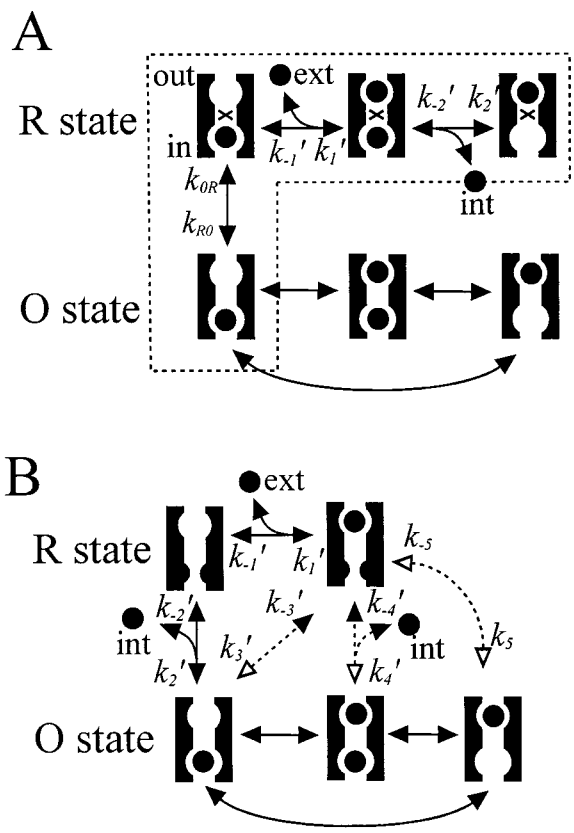


FIGURE 8 Working models of intrinsic filter region gating. In both figures, schematic representations of the various $K^+$-bound forms of the channel's selectivity filter proposed to underlie the distribution between the R (*top rows*) and O (*bottom rows*) states are shown. Circles represent bound, internal ("int"), or external ("ext") $K^+$ ions. Voltage-dependent rates (i.e., those involving $K^+$ binding) are indicated by apparent rate constants marked with apostrophes. See Discussion for detailed descriptions of both models. (*A*) Intra-filter-gate mechanism. In this scheme, the R state is determined by the closing of an intra-filter "gate." The dashed box represents the portion of model used for predictions of *G/V* relationships. (*B*) Collapsed filter mechanism. A partial collapse of the filter's inner binding site underlies the R state here. Transitions that occur too rarely to be significant in this scheme are designated by hollow arrowheads.

## Postulation of specific mechanisms of R-state gating

Although our data do not specifically support a particular mechanism, we nonetheless speculate how the $\Delta\mu_{K^+}$-dependent R state can, as we conclude, be an intrinsic property of the channel filter region. At least two distinct mechanisms can be envisioned: an intra-filter-gate mechanism and an altered-binding mechanism. An intra-filter gating mechanism (Fig. 8 *A*) is the simpler to envision. As ascertained above, the inner and outer sites must be exposed to their respective solutions in the R state, dictating that an R-state gate would have to reside between the two sites rather than on either side. $\Delta\mu_{K^+}$ dependence could be explained if $K^+$ binding to the outer site blocked R/O transition. For example, the outer site may need to contract slightly during R/O transition, which would be antagonized by bound $K^+$. $K^+$ bound to the outer site would thus lock the channel in the R state and inner $K^+$ binding would conversely favor R to O transition by antagonizing outer site binding through electrostatic repulsion. The low $Q_{10}$ of R to O transition and the difficulty envisioning a closed intra-binding-site gate leaving both sites intact argue against the gate being a simple physical occlusion/deocclusion of the pore, because that would presumably require substantial rearrangement of the local structure. An appealing alternative is that gating instead relies on a change in the dielectric surface between the sites. The two binding sites of the KcsA (and presumably the Tok1 filter) are separated by several $K^+$ ionic radii. An ion hopping between the sites, an obligatory step during conduction, will thus be substantially unbound from either site and largely dehydrated at some intermediate point. The negative dielectric environment of the pore surface in this region (Doyle et al., 1998) must thus be the key to maintaining a low activation barrier to hopping and therefore high throughput. A realignment of oxygen groups away from or amide groups toward the pore lining could in theory underlie a conformationally subtle R-state gate.

The altered binding mechanism (Fig. 8 *B*) requires a somewhat more complex set of assumptions. In this scheme, the inner site is capable of dwelling both in an O state and, in the absence of bound $K^+$, an R state, which has a higher energetic barrier against $K^+$ binding. Such behavior could

reflect a partial collapse of the filter, somewhat analogous to the mechanism that has been proposed to underlie C-type inactivation of *Shaker* channels (Kiss and Korn, 1998). Return to the O form would involve an induced-fit squeezing open of the site by the binding of energetic $K^+$ from the inner solution. The R to O transition rate of $10^4$ $s^{-1}$ should be consistent with ~1 of 1000 ions that collide with the O state binding site with sufficient kinetic energy to dehydrate during conductance, having sufficient energy to dehydrate and reopen the collapsed R-state site. In order to account for $\Delta\mu_{K^+}$ dependence, several constraints must be presumed. First, a prohibitive barrier must exist between the R and O state when the inner site is unoccupied (i.e., the $k_5$ and $k_{-5}$ transitions will be irrelevantly rare). Mechanistically, such an effect implies a requisite transitional conformation that is strongly facilitated by $K^+$ binding. Second, $K^+$ bound to the outer site must preclude the induced-fit binding of $K^+$ to the inner site (i.e., $k_4$ is disallowed). This could be accounted for by electrostatic repulsion. Finally, transfer from the outer to the inner R-state site ($k_3$) must be disallowed. This restriction is consistent with the premise stated above that only ions with exceptional kinetic energies can squeeze open the inner R-state site. Accepting these constraints, $\Delta\mu_{K^+}$ dependence follows naturally with the evacuated form of the R state being the $\Delta\mu_{K^+}$ sensor per se. Binding of $K^+$ to the outer site will maintain the channel in the R state, whereas induced binding to the inner site will return the channel to the O state. Although more complex than the intra-filter gating scheme, this collapsed-filter mechanism readily accounts for the low $Q_{10}$ of R to O activation because the rate-limiting step is $K^+$ binding.

It is notable that a consequence of both models is that the channel should continuously cycle between the O and R state when the driving force is outward, which is consistent with the observed rapid flickery behavior of Tok1 (Gustin et al., 1986). Furthermore, both models are consistent with the observation that external $Rb^+$ and $Cs^+$ affect Tok1's steady-state rectification similar to $K^+$ (Bertl et al., 1998) if it is assumed that both of these $K^+$-like ions can bind to the outer site.

The theoretical feasibility of the intra-site-gating scheme was tested by determining whether a mathematical model of it could describe the observed steady-state *G/V* relationship in symmetrical $K^+$ with reasonable parameters, and whether these parameters could then predict the *G/V* relationship in nonsymmetrical conditions. To facilitate such an analysis, the multiple forms of the O state were ignored and the fully evacuated form of the R state was eliminated to make it possible to apply a simple equilibrium-based analysis of the relative distributions between the various states (The simplified scheme used here is indicated by the dashed box in Fig. 8 *B* and described in detail in the Appendix). Voltage and $K^+$ dependence results from binding to the inner and outer sites, which were arbitrarily positioned ⅓ the way into the membrane's electrical field from the inner and outer solutions (see Appendix). It was presumed that $K^+$ binding to both sites occurs at $3.4 \times 10^7$ $s^{-1}$ in the absence of applied voltage (based on the observed unitary conductance in 100 mM $K^+$ (Gustin et al., 1986) and the assumption that binding is the rate-limiting step during transport), and that R/O transition occurs at voltage-independent rates of 0.1 ms (based on the observed R to O transition rates). With these simplifications and assumptions, the symmetrical *G/V* relationship can be accurately described (Fig. 9 *B, middle trace*) if unbinding from the inner and outer sites in the face of electrostatic repulsion occur ~1000 and 20-fold faster, respectively, than binding. The conclusion that unbinding from the inner site of the R form ($k'_2$ in Fig. 8 *B*) must occur ~50-fold faster than unbinding from the outer site ($k'_{-1}$) could be interpreted as indicating that the unfavorable dielectric environment proposed to underlie the R state also weakens the binding to the inner site. These same parameters can be used to reasonably predict the nonsymmetrical *G/V* relationships (Fig. 9 *B*, *left* and *right* traces, see Appendix for details of calculations). Although the overall prediction of the waveform of the *G/V* relationship is accurate, the predicted outward conductance in 14 mM internal $K^+$ is larger than the observed conductance, possibly reflecting an unaccounted low-$K^+$-dependent effect on unitary conductance. Despite the clear speculative nature of the model, it is intriguing that it can describe the observed *G/V* relationships with reasonable parameters.

## The C states

The high temperature dependence of activation from the C states and apparent key role of the inner mouth of the pore in C-state dwell lead us to conclude that a gross conformational occlusion of the inner pore likely underlies these states. The effect of $V_m$ and external but not internal $K^+$ indicate that this rearrangement results from binding of $K^+$ to an external-only accessible allosteric site within the membrane's electrical field. It is appealing for the sake of structural simplicity to model this site as being the filter itself. Unfortunately, the filter is not a viable candidate as such an allosteric site because almost all of the channels will have $K^+$ bound to the outer site below $E_K$ in our R state

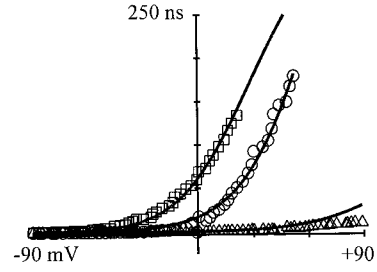


FIGURE 9 Predictions (*solid lines*) of observed (*symbols*) *G/V* relationships in 140 $K_{in}$/14 $K_{out}$ (□), 140 $K_{in}$/140 $K_{out}$ (○), and 14 $K_{in}$/14 $K_{out}$ (△) based on an equilibrium-based prediction of $P_O$ of a simplified scheme of the R state shown within the dashed box in Fig. 8 *A*. The symmetrical trace was used to derive unbinding parameters and maximal conductance, and these parameters were then used to predict the *G/V* relationships in the nonsymmetrical conditions (see Discussion and Appendix).

models, yet the distribution between R and C changes significantly in this voltage range.

Instead, an additional nonfilter allosteric binding site must be proposed. To account for the steep dependence of C dwell on voltage, binding to either a single site buried deeply within the electrical field or several partially buried sites would determine C dwell. A single-site scheme would require a canal crossing much of the membrane's field parallel to the channel pore. The solid lines in Fig. 7 *B* represent the predicted C distribution assuming an allosteric binding site with a $K_d$ of 0.25 $M^{-1}$ located 60% of the electrical distance across the membrane. A multi-site model is structurally more economical because these sites could be located in the outer vestibule of the channel pore, but would require at least eight independent binding sites buried 10% into the field to adequately account for the voltage dependence of C dwell (fitting not shown). In either case, binding to the allosteric site would be weaker than binding to the filter site to account for the significant dwell in R at voltages mildly negative to $E_K$.

## SUMMARY

In summary, we conclude that there is now substantial evidence that the R and C states reflect fundamentally distinct properties of Tok1. The $\Delta\mu_{K^+}$-dependence of the R state strongly indicates that it reflects an intrinsic property of the channel filter region. The C state, however, most likely results from a conformational occlusion of the inner mouth of the permeation pathway in response to binding $K^+$ to an externally accessible allosteric binding site. Other factors that may be important in Tok1's regulation, such as pH and phosphorylation (Bertl et al., 1998; Lesage et al., 1996), will need to be incorporated into any models considering Tok1's true physiological functioning. Nonetheless, our findings limit the scope of the mechanisms that can reasonably be proposed to account for Tok1's behavior and facilitate directing future investigations of this highly complex ion channel.

## APPENDIX

### Calculation of *G/V* relationships based on an intra-filter-gate model of the R state

The overall model in Fig. 8 *A* had to be simplified, and only the states shown within the dotted box were considered to allow an equilibrium-based prediction of the *G/V* relationship. The various $K^+$-bound forms of the O state were treated as a single "O" state because the open conducting channel is not in equilibrium in the presence of a $K^+$ electrochemical gradient. Such a simplification will, if anything, underestimate the effect of $\Delta\mu_{K^+}$ on *G* in this scheme because the channel should remain primarily in the outer bound form (which is incapable of migrating to R) when open in the presence of an outward $\Delta\mu_{K^+}$ if it is assumed that the rate-limiting step during conduction is the binding of $K^+$ to the filter. The evacuated form of the R state was also ignored (not shown in Fig. 8 *A*) because it is most likely extremely rare due to the slow rate of $K^+$ unbinding in the absence of repulsion from another bound ion (Baukrowitz and Yellen, 1996) and its inclusion would complicate the analysis.

The simplified forms used in this analysis are referred to as $R_I$, $R_{IO}$, $R_O$ corresponding to the inner-only-bound-, dual-bound-, and outer-only-bound- forms of the R state and O, the conducting open state. Because the R-state behavior alone primarily accounts for the steady-state *G/V* relationship (Loukin et al., 1997), the dependence of steady-state ensemble conductance (*G*) on the distribution between the three forms of Fig. 8 *A* can be described by:

$$G = G_{max}P_O = G_{max}\frac{[O]}{([O] + [R_I] + [R_{IO}] + [R_O])} \quad (1)$$

At equilibrium, the relative distribution among the three states should be:

$$O = \frac{k_{RO}R_I}{k_{OR}} \quad (2)$$

$$R_I = \frac{k_{OR}O + k'_{-1}R_{IO}}{k_{RO} + k'_1[K^+]_{ext}} \quad (3)$$

$$R_{IO} = \frac{k'_1[K^+]_{ext}R_1 + k'_{-2}[K^+]_{int}R_O}{k'_{-1} + k'_2} \quad (4)$$

$$R_O = \frac{k'_2R_{IO}}{k'_{-2}[K^+]_{int}} \quad (5)$$

Where $k_{RO}$ and $k_{OR}$ refer to the presumed voltage-independent R to O transitions and the apparent rate constants ($k'_1$, $k'_{-1}$, $k'_2$, $k'_{-2}$) describe the voltage-dependent binding and unbinding of $K^+$ to the filter, as shown in Fig. 8 *A*. Their voltage dependence is described by:

$$k'_1 = k_1 \exp(-\delta_1 V/RT) \quad (6)$$

$$k'_{-1} = k_{-1} \exp(\delta_1 V/RT) \quad (7)$$

$$k'_2 = k_2 \exp(-\delta_2 V/RT) \quad (8)$$

$$k'_{-2} = k_{-2} \exp(\delta_2 V/RT) \quad (9)$$

where $k_x$ describes the intrinsic rates in the absence of a voltage field, and $\delta_1$ and $\delta_2$ are the fractional electrical distances between the outer binding site and the external solution or the inner binding site and the internal solution, respectively. *V* is the membrane potential ($V_m$) and *R* and *T* have the standard meanings.

It was assumed that the binding of $K^+$ to the filter is the rate-limiting step accounting for the observed 20 pS unitary conductance of Tok1 in 100 mM $K^+$ (Gustin et al., 1986) (i.e., $k_1 = k_{-2} = 3.4 \times 10^7\ s^{-1}$), that the two binding sites are located a third the way into the membrane's electrical field from the inner and outer solutions, respectively (i.e., $\delta_1 = \delta_2 = 0.33$) and that the R/O transitions take 100 $\mu$s in either direction (i.e., $k_{RO} = k_{OR} = 10^4\ s^{-1}$). The observed symmetrical *G/V* relationship (Fig. 9, ○) was fit to Eqs. 1–9 utilizing these assumptions by arbitrarily setting $R_{IO}$ to 1 and floating $k_{-1}$, $k_2$, and $G_{max}$ using nonlinear regression analysis of Sigma Plot 4.0.

The parameters derived from the fit of the symmetrical $K^+$ trace were used to predict the *G/V* plots under asymmetrical conditions. The resultant *G/V* plots had to be corrected for the rectifying effect of differential permeant ion concentration by using the Goldmann-Hodgkin-Katz (GHK) current equation for $K^+$ ions independently crossing a membrane with a linearly decaying electrical field (Hille, 1992):

$$I = P\frac{EF^2}{RT}\frac{[K^+]_{int} - [K^+]_{ext}\exp(-FE/RT)}{1 - \exp(-FE/RT)} \quad (10)$$

where *P* is the channel-containing membrane's permeability to $K^+$. This relationship predicts that the GHK effect on rectification caused by a

10-fold reduction of external $K^+$ will be:

$$\frac{G_{140/14}}{G_{140/140}} = \frac{I_{140/14}/(V + 0.058)}{I_{140/140}/V} = \frac{V}{(V + 0.058)} \frac{1 - 0.1\exp(-FV/RT)}{1 - \exp(-FV/RT)} \quad (11)$$

where $G_{140/14}$ and $G_{140/140}$ are the predicted ensemble channel conductances in 140 mM $[K^+]_{int}$/14 mM $[K^+]_{ext}$ and symmetrical 140 mM $[K^+]$, respectively, at $P_O = 1$, and $I_x$ values have analogous meanings. Reducing $[K^+]_{int}$ 10-fold is likewise predicted to affect conductance by:

$$\frac{G_{14/140}}{G_{140/140}} = \frac{I_{14/140}/(V - 0.058)}{I_{140/140}/V} = \frac{V}{(V - 0.058)} \frac{0.1 - \exp(-FV/RT)}{1 - \exp(-FV/RT)} \quad (12)$$

In addition to these corrections, $G_{max}$ in the 14 mM external $K^+$ trace had to be standardized (because the data come from a different patch) by equating the predicted trace with the actual trace at 0 mV. This linear correction was ~20%.

We thank Ching Kung, G. A. Robertson and co-workers for providing *Xenopus* oocytes and Drs. P. Blount and C. Palmer for critical reading of the manuscript.

This work was partially supported by National Institutes of Health Grants GM 22714 and 36386.

## REFERENCES

Alvarado, F., E. Brot-Laroche, L. H. M. H. Murer, and G. Stange. 1979. The effect of harmaline on intestinal sodium transport and on sodium-dependent D-glucose transport in brush-border membrane vesicles from rabbit jejunum. *Pflugers Arch.* 382:35–41.

Baukrowitz, T., and G. Yellen. 1996. Use-dependent blockers and exit rate of the last ion from the multi-ion pore of a $K^+$ channel. *Science.* 271:653–656.

Beam, K. G., and P. L. Donaldson. 1983. A quantitative study of potassium channel kinetics in rat skeletal muscle from 1 to 37 degrees C. *J. Gen. Physiol.* 81:485–512.

Bertl, A., H. Bihler, J. D. Reid, C. Kettner, and C. L. Slayman. 1998. Physiological characterization of the yeast plasma membrane outward rectifying $K^+$ channel, *DUK1* (*TOK1*), in situ. *J. Membr. Biol.* 162: 67–80.

Chen, T. Y., and C. Miller. 1996. Nonequilibrium gating and voltage dependence of the ClC-0 $Cl^-$ channel. *J. Gen. Physiol.* 108:237–50.

Chiu, S. Y., H. E. Mrose, and J. M. Ritchie. 1979. Anomalous temperature dependence of the sodium conductance in rabbit nerve compared with frog nerve. *Nature.* 279:327–328.

Collins, C. A., and E. Rojas. 1982. Temperature dependence of the sodium channel gating kinetics in the node of Ranvier. *Q. J. Exp. Physiol.* 67:41–55.

Doyle, D. A., J. M. Cabral, R. A. Pfuetzner, A. Kuo, J. M. Gulbis, S. L. Cohen, B. T. Chait, and R. Mackinnon. 1998. The structure of the potassium channel: molecular basis of $K^+$ conduction and selectivity. *Science.* 280:69–77.

Dudel, J., and R. Rudel. 1970. Voltage and time dependence of excitatory sodium current in cooled sheep Purkinje fibres. *Pflugers Arch.* 315: 136–158.

Frankenhauser, B., and L. E. Moore. 1963. The effect of temperature on the sodium and potassium permeability changes in myelinated nerve fibres of *Xenopus laevis. J. Physiol.* (*Lond.*) 169:431–437.

Gustin, M. C., B. Martinac, Y. Saimi, M. R. Culbertson, and C. Kung. 1986. Ion channels in yeast. *Science.* 233:1195–1197.

Hille, B. 1992. Ionic Channels of Excitable Membranes. 2nd Ed. Sinauer Associates, Inc., Sunderland, MA.

Hodgkin, A. L., and B. Katz. 1949. The effect of temperature on the electrical activity of the giant axon of the squid. *J. Physiol.* (*Lond.*) 109:240–249.

Ketchum, K. A., W. J. Joiner, A. J. Sellers, L. K. Kaczmarek, and S. A. Goldstein. 1995. A new family of outwardly rectifying potassium channel proteins with two pore domains in tandem. *Nature.* 376:690–695.

Kiss, L., D. Immke, J. LoTurco, and S. J. Korn. 1998. The interaction of $Na^+$ and $K^+$ in voltage-gated potassium channels. Evidence for cation binding sites of different affinity. *J. Gen. Physiol.* 111:195–206.

Kiss, L., and S. J. Korn. 1998. Modulation of C-type inactivation by $K^+$ at the potassium channel selectivity filter. *Biophys. J.* 74:1840–1849.

Lesage, F., E. Guillemare, M. Fink, F. Duprat, M. Lazdunski, G. Romey, and J. Barhanin. 1996. A pH-sensitive yeast outward rectifier $K^+$ channel with two pore domains and novel gating properties. *J. Biol. Chem.* 271:4183–4187.

Loukin, S. H., B. Vaillant, X.-L. Zhou, E. P. Spalding, C. Kung, and Y. Saimi. 1997. Random mutagenesis reveals a region important for gating of the yeast $K^+$ channel, Ykc1. *EMBO J.* 16:4817–4825.

Miosga, T., A. Witzel, and F. K. Zimmermann. 1994. Sequence and function analysis of a 9.46 kb fragment of *Saccharomyces cerevisiae* chromosome X. *Yeast.* 10:965–973.

Moore, L. E. 1971. Effect of temperature and calcium ions on rate constants of myelinated nerve. *Am. J. Physiol.* 221:131–137.

Reid, J. D., W. Lukas, R. Shafaatian, A. Bertl, C. Scheurmann-Kettner, H. R. Guy, and R. A. North. 1996. The *S. cerevisiae* outwardly-rectifying potassium channel (*DUK1*) identifies a new family of channels with duplicated pore domains. *Receptors and Channels.* 4:51–62.

Schauf, C. L. 1973. Temperature dependence of the ionic current kinetics of *Myxicola* giant axons. *J. Physiol.* (*Lond.*) 235:197–205.

Schreibmayer, W., H. A. Lester, and N. Dascal. 1994. Voltage clamping of *Xenopus laevis* oocytes utilizing agarose-cushion electrodes. *Pflugers Arch.* 426:453–458.

Starkus, J. G., L. Kuschel, M. D. Rayner, and S. H. Heinemann. 1997. Ion conduction through C-type inactivated *Shaker* channels. *J. Gen. Physiol.* 110:539–550.

Starkus, J. G., L. Kuschel, M. D. Rayner, and S. H. Heinemann. 1998. Macroscopic $Na^+$ currents in the "nonconducting" *Shaker* potassium channel mutant W434F. *J. Gen. Physiol.* 112:85–93.

Vergani, P., T. Miosga, S. M. Jarvis, and M. R. Blatt. 1997. Extracellular $K^+$ and $Ba^{2+}$ mediate voltage-dependent inactivation of the outward-rectifying $K^+$ channel encoded by the yeast gene *TOK1. FEBS Lett.* 405:337–344.

Zhou, X. L., B. Vaillant, S. H. Loukin, C. Kung, and Y. Saimi. 1995. *YKC1* encodes the depolarization-activated $K^+$ channel in the plasma membrane of yeast. *FEBS Lett.* 373:170–176.